Radio-Wave Communication With Chaos

CHAO BAI[1], HAI-PENG REN[1], (Member, IEEE), WU-YUN ZHENG[2], AND CELSO GREBOGI[2,3]
[1]Xi'an Key Laboratory of Intelligent Equipment, Xi'an Technological University, Xi'an 710021, China
[2]Shaanxi Key Laboratory of Complex System Control and Intelligent Information Processing, Xi'an University of Technology, Xi'an 710048, China
[3]Institute for Complex Systems and Mathematical Biology, University of Aberdeen, Aberdeen AB24 3UE, U.K.

Corresponding author: Hai-Peng Ren (renhaipeng@xaut.edu.cn)

ABSTRACT Chaotic signals require very wide bandwidth to be transmitted in a practical channel, which is difficult for the practical transducer or antenna to convert such a broadband signal. To address this problem, in this work, Chaotic Shape-forming Filter (CSF) is used to obtain the baseband signal, and the corresponding matched filter is used at the receiver to maximize the signal-to-noise ratio. At the same time, the symbol judgment threshold determined by the chaos properties is used to reduce the Inter-Symbol Interference (ISI) effect. Simulations and virtual channel experiments show that the radio-wave communication system using chaos is inferior to the conventional radio-wave communication system using Square Root Raised Cosine (SRRC) shape-forming filter in a single path channel. This is because SRRC eliminates ISI in single path, but CSF does not. However, the chaos-based communication with anti-multipath decoding algorithm shows significantly better Bit Error Rate (BER) performance than the traditional communication system using SRRC and a minimum mean square error (MMSE) channel equalization in a multipath channel. This work shows the potential application prospect of chaos-based communication in future 5G or 6G engineering communication systems.

INDEX TERMS Chaotic communication, decoding, multipath channels, radio-wave communication.

I. INTRODUCTION

Chaos, having a random like deterministic dynamics, has many properties suitable for communication applications, such as wide spectrum, sensitivity to initial data and pulse-like auto-correlation. The realization of chaos control [1] and synchronization [2] has laid the foundation for the application of chaotic signals. Hayes *et al*. used perturbation control to encode information sequence into chaotic signals that were used in communication [3]. Since then, many communication methods have been proposed, such as Chaos Masking [4], [5], Chaos Modulation [6], [7], Chaos Spread Spectrum [8], [9], Chaos Shift Keying [10], [11] and their improvements [12]–[16].

The research of chaotic communication was originally focused on the security performance in ideal channels with white noise. With further developments, the research hotspot has gradually turned to the use of chaos to improve the performance of traditional communication systems. Since Argyris *et al*. used chaotic signals to improve the bit

transmission rate in the optical fiber communication system [17], the research on communication with chaos shifted from ideal channels to practical communication channels. Compared with the ideal channel, the wireless channel is a practical channel subjected to more complex constraints, such as multi-path propagation and Doppler shift [18]. Whether chaos could be applied to wireless channel became a basic and practical problem. Recent work showed that the information in chaotic signal is preserved after transmitted through wireless channel [19]. At the same time, experimental circuit encoding and decoding methods for wireless communication were designed to validate the theoretical predictions [20]. Besides these advances, other advantages for using chaos into communication have been reported recently, including the use of simple matched filter to achieve the maximum signal to noise ratio [21], [22], and a decoding threshold using chaos property to relief Inter-Symbol Interference (ISI) caused by multi-path propagation [23], [24]. All these progresses pushed the research forward to the practical application of chaos in communication systems. However, it is very difficult for the current available transducers or antennas to convert the chaotic signal into the media waveform (radio-wave or

---

The associate editor coordinating the review of this manuscript and approving it for publication was Jenny Mahoney.
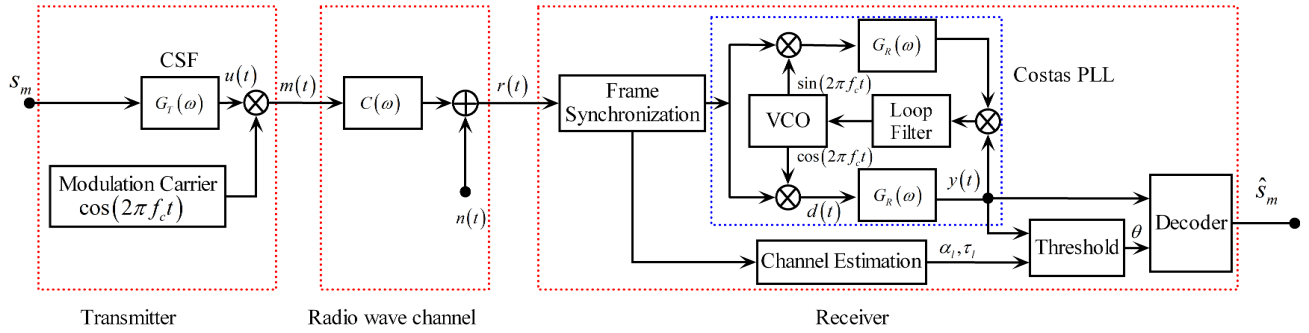
FIGURE 1. Block diagram of radio wave communication system.

acoustic signal). This is because the chaotic signal possesses wide spectrum bandwidth, while the transducers, antennas and the associate amplifiers have relatively narrow bandwidth. This fact prevents the chaos application in practical communication systems. The coping with this obstacle is the key for future research work on communication with chaos.

In this paper, we show that the simplest way to solve the above obstacle is by using a Chaotic Shape-forming Filter (CSF) to replace the conventional shape-forming filter. Using radio-wave communication system as example, we compare the performance of the radio wave communication system using the chaotic shape-forming filter and the corresponding matched filter with the conventional radio wave communication system. In such a way, we capitalize on the advantages that chaotic signal provides to improve the practical performance of conventional communication system. The features and contributions of this work are: (1) In the proposed communication system framework, a chaotic shape-forming filter is used to replace the conventional shape forming filter and a corresponding matched filter is used to replace the traditional low-pass filter in the Costas Phase Locked Loop (PLL). It is completely compatible with the traditional radio wave communication system hardware. (2) This work validates the chaotic baseband wireless communication method in a radio wave communication test platform, combining with the anti-multipath decoding algorithm in [23]. The system achieves higher reliability than the conventional radio wave communication system. (3) It is the first time being reported and demonstrated experimentally that the chaotic shape-forming filter is inferior to the conventional Square Root Raised Cosine (SRRC) filter in single path radio wave communication.

The remaining of the paper is organized as follows. The radio-wave communication system configuration using chaos is presented in Sec. II. The system working principle of the proposed method is reported in Sec. III. In Sec. IV, the decoding threshold is introduced. Simulation and experimental results are reported in Sec. V, verifying the validity and superiority of the proposed method. Finally, some concluding remarks are given in Sec. VI.

II. RADIO-WAVE COMMUNICATION SYSTEM CONFIGURATION

In digital communication systems, the time-domain waveform of the transmitted information is treated as a rectangular pulse, which is difficult to transmit because of the broadband requirement. The shape-forming filter is used to compress the input signal bandwidth, and to convert the information bit into a baseband signal waveform suitable for the channel transmission. In this work, a chaotic shape-forming filter replaces the conventional shape-forming filter to generate the baseband signal. The baseband signal spectrum is moved to the bandwidth range by linear modulation so that it is fit for the radio wave channel transmission. Figure 1 shows the radio wave communication system block diagram, where $G_T(\omega)$, $C(\omega)$, and $G_R(\omega)$ represent the shape-forming filter, wireless transmission channel, and the matched filter, respectively; the binary information bits s_m pass through the chaotic shape-forming filter to form the baseband signal $u(t)$, and the modulated carrier is used to modulate the baseband signal $u(t)$ to obtain the radio frequency band signal $m(t)$. After the transmitted signal passes through the wireless channel, the frame synchronization and channel estimation are conducted using the Synchronization (Sync) probe signal; the carrier synchronization is implemented by using a Costas PLL to obtain demodulation signal $d(t)$ and filter output signal $y(t)$. Then, the decode threshold θ is obtained by sending the filter output signal and the parameters of the channel estimation to the anti-multipath threshold calculation algorithm. Finally, the decoder is used to decode the information bits $\hat{s}_m$ from the calculated threshold θ.

III. SYSTEM WORKING PRINCIPLE

From Fig. 1, we recognize that the system configuration of chaos wireless communication is precisely the conventional radio wave communication system configuration. Therefore, we simply replace the shape-forming filter with the chaotic one and also replace the matched filter accordingly. In the following, the principle of radio wave communication system using the properties of chaos is elaborated.
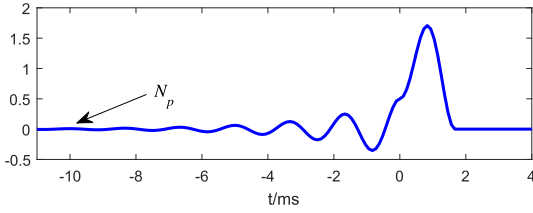
FIGURE 2. Time-domain waveform of the basis function $p(t)$, where the base frequency is $f = 0.6\ kHz$ and the sampling frequency is $f_S = 9.6\ kHz$.

In our proposed radio-wave communication system, a basis function is displayed in Eq. (1) and its time domain waveform is shown in Fig. 2. In fact, the basis function given by Eq. (1) [21], [24] is used to encode the source code stream (information) by using the convolution of the basis function with the bipolar information bit [25]. By this way, the information is encoded into the chaotic baseband signal.

$$p(t) = \begin{cases} \left(1 - e^{-\frac{\beta}{f}}\right) e^{\beta t} \left(\cos(\omega t) - \frac{\beta}{\omega}\sin(\omega t)\right), \\ \qquad t < 0 \\ 1 - e^{\beta\left(t - \frac{1}{f}\right)}\left(\cos(\omega t) - \frac{\beta}{\omega}\sin(\omega t)\right), \\ \qquad 0 \le t < \frac{1}{f} \\ 0, \\ \qquad t \ge \frac{1}{f}, \end{cases} \quad (1)$$

where $\omega = 2\pi \cdot f$ and $\beta = f \cdot \ln 2$ are parameters, and f is the base frequency of the chaotic signal used to adjust the data transmission rate in the baseband signal. The basis function is decaying fast in the backward direction and N_p, a positive integer, denotes the time instant at which the basis function amplitude can be neglected, that is, if $t < -N_p$ then $p(t) \approx 0$. From Fig. 2, the requirement is satisfied for $N_p = 6/f = 10ms$. The chaotic baseband signal is generated as Eq. (2) by convoluting the information bit, s_m, with the basis function, as depicted by $G_T(\omega)$ in Fig. 1. The shape-forming filter output, $u(t)$, is given by

$$u(t) = \sum_{m=-\infty}^{\infty} s_m \cdot p(t - \frac{m}{f}), \quad s(t) = s_{\lfloor t \cdot f \rfloor} \quad (2)$$

where $s_m = \pm 1$, $\lfloor t \cdot f \rfloor$ is the closest integer in the downward direction. It means that the chaotic baseband waveform can be generated by a convolution between the information bits and the basis function in Eq. (2) rather than by the integration of the differential equation, as equation (1) in [16]. The filter in Eq. (2) is not only compatible with the practical communication equipment without an extra electronic circuit, but it is also easy to implement yielding an improved communication performance. Given a symbol sequence,

$$[1 - 11 - 11, 11 - 111, -111 - 1 - 1, 1 - 1 - 1 - 11,$$
$$-111 - 11, -1 - 1 - 1 - 11],$$

the shape-forming filter output is shown in Fig. 3(a), where the red dash line shows the information sequence and the blue
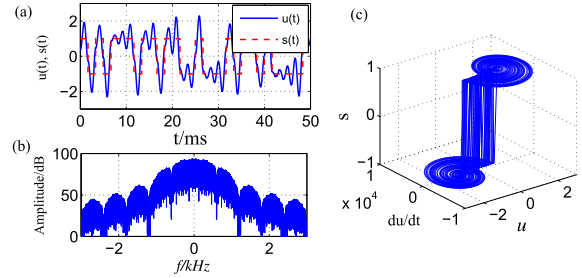

FIGURE 3. Chaotic shape-forming filter output and its properties with $f = 0.6\ kHz$ and the sampling frequency $f_S = 9.6\ kHz$; (a) Filter output and information symbol; (b) The spectrum of the filter output; (c) The three dimensional phase plot of the states and information.

solid line is the shape-forming filter output. Figure 3(b) shows the spectrum of the shape-forming filter output. Figure 3(c) is the three dimensional phase space plot of the states and the information. As can be seen from Fig. 3(b), the chaotic signal has a rich low-frequency component. In order to meet the bandwidth requirement of the radio wave channel transmission, the spectrum of the baseband signal is shifted to the required channel bandwidth range using linear modulation (referred to as Double Side Band Suppression Carrier, DSB-SC) to obtain the transmitted signal, $m(t)$, as

$$m(t) = u(t) \cdot \cos(2\pi f_c t), \quad (3)$$

where f_c is the carrier frequency.

The wireless channel mathematical model [26] is given by

$$h(t) = \sum_{l=0}^{L-1} \alpha_l \delta(t - \tau_l) + n(t), \quad (4)$$

where $\delta(\cdot)$ is Dirac function, α_l and τ_l are the attenuation coefficient and the delay-time for the lth multi-path in the channel, respectively, and $n(t)$ is the Gaussian noise.

At the receiver, the frame synchronization is identified by using a correlation operation between the received signal and the Sync probe signal. We can find from the PLL in Fig. 1 that the low-pass filters are replaced by the matched filters $G_R(\omega)$. Therefore, the demodulation signal and the filter output signal are obtained by passing through the received signal into the Costas PLL. The demodulation signal is given by

$$d(t) = m(t)\cos(2\pi f_c t)$$
$$= \frac{1}{2}u(t) + \frac{1}{2}u(t)\cos(4\pi f_c t). \quad (5)$$

The corresponding matched filter, with impulse response given by $g(t) = p(-t)$, is used to filter out the high frequency term of Eq. (5), due to its low-pass characteristic, and to maximize the signal-to-noise ratio, as shown by

$$y(t) = g(t) * d(t), \quad (6)$$

where '∗' denotes convolution.

The matched filter output signal waveform $y(t)$ and its spectrum are shown in Fig. 4. Subplots (a) and (c) in Fig. 4 are the matched filter output in the single-path and the double-path channels, respectively; the subplots (b) and (d) in Fig. 4
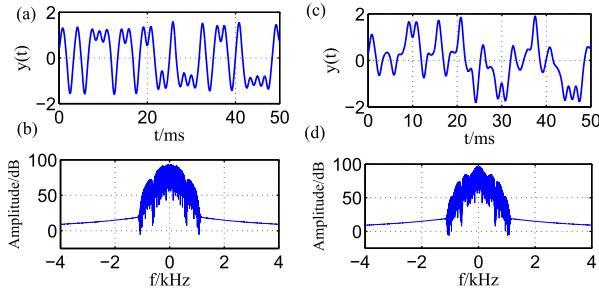
FIGURE 4. The output signal waveform of the matched filter and its spectrum, where the base frequency is $f = 0.6$ *kHz*, sampling frequency is $f_s = 9.6$ *kHz*, carrier frequency is $f_c = 1.8$ *kHz*, and signal to noise ratio is $SNR = 20$ *dB*; (a) Filter output for the single path; (b) The spectrum of the signal in (a); (c) The filter output for the two paths; (d) The spectrum of the signal in (c).

are the corresponding spectra of the filter output signal in subplots (a) and (c), respectively. The sampled value using sampling interval set at T_s (T_s is the symbol period) in the decoder gets the maximum signal-to-noise ratio.

IV. THE ANTI-MULTIPATH ALGORITHM

In wireless channel, ISI caused by multi-path propagation is unavoidable. In traditional wireless communication systems, the ISI effect is decreased by using complicated channel equalization methods. Due to a property of the chaotic signal, ISI effect can be decreased by using the proper decoding threshold [23]. Here, the method is briefly explained as follows.

In our proposed communication system, the signal received by the receiver is given by

$$
\begin{aligned}
r(t) &= h(t) * u(t) + n(t) \\
&= \sum_{l=0}^{L-1} \alpha_l \sum_{m=-\infty}^{\infty} s_m p\left(t - \tau_l - \frac{m}{f}\right) + n(t), \quad (7)
\end{aligned}
$$

where $n(t)$ is Gaussian noise. Then the matched filter output is given by

$$
\begin{aligned}
y(t) &= g(t) * r(t) \\
&= \int_{-\infty}^{\infty} p(-\tau) r(t - \tau) d\tau \\
&= \sum_{l=0}^{L-1} \alpha_l \sum_{m=-\infty}^{\infty} s_m \left(\int_{-\infty}^{\infty} p(\tau) p\left(\tau - t \right. \right. \\
&\quad \left. \left. + \tau_l + \frac{m}{f}\right) d\tau \right) \\
&\quad + \int_{-\infty}^{\infty} p(\tau - t) n(\tau) d\tau. \quad (8)
\end{aligned}
$$

Sampling $y(t)$ at frequency f, yields

$$
\begin{aligned}
y_n &= \sum_{l=0}^{L-1} \alpha_l \sum_{m=-\infty}^{\infty} s_m \left(\int_{-\infty}^{\infty} p(\tau) p\left(\tau + \tau_l + \frac{m-n}{f}\right) d\tau \right) \\
&\quad + \int_{-\infty}^{\infty} p\left(\tau - \frac{n}{f}\right) n(\tau) d\tau
\end{aligned}
$$

$$
\begin{aligned}
&= \sum_{l=0}^{L-1} \sum_{m=-\infty}^{\infty} s_m C_{l,m-n} + W \\
&= \sum_{l=0}^{L-1} s_n C_{l,0} + \sum_{l=0}^{L-1} \sum_{\substack{m=-\infty \\ m \neq n}}^{\infty} s_m C_{l,m-n} + W \\
&= s_n P + I + W, \quad (9)
\end{aligned}
$$

where P is the sum of the multi-path power for s_n, I is the interference from other symbols in the multi-path, and W is the noise effect. $C_{l,j}$ is the sampled value of the lth multi-path at the jth instant, given by

$$
C_{l,j}
$$

$$
= \begin{cases}
\alpha_l D \left(2 - e^{-\frac{\beta}{f}} - e^{\frac{\beta}{f}}\right) (A \cos(\omega \tau_l) + B \sin(\omega \tau_l)), \\
\qquad \left| \tau_l + \dfrac{j}{f} \right| \geq \dfrac{1}{f} \\[2ex]
\alpha_l \left\{ \begin{array}{l}
A\left(D\left(2 - e^{-\frac{\beta}{f}}\right) - D^{-1}e^{-\frac{\beta}{f}}\right) \cos(\omega \tau_l) + \\
B\left(D\left(2 - e^{-\frac{\beta}{f}}\right) + D^{-1}e^{-\frac{\beta}{f}}\right) \sin(\omega \tau_l) + 1 \\
- |\tau_l f + j|
\end{array} \right\}, \\
\qquad 0 \leq \left| \tau_l + \dfrac{j}{f} \right| < \dfrac{1}{f}
\end{cases}
$$

$$(10)$$

where $A = \dfrac{(\omega^2 - 3\beta^2)f}{4\beta(\omega^2 + \beta^2)}$, $B = \dfrac{(3\omega^2 - \beta^2)f}{4\omega(\omega^2 + \beta^2)}$ and $D = e^{-\beta}\left|\tau_l + \frac{i}{f}\right|$.

If there would be no I in Eq. (9), then the symbol s_n could be decoded by comparing the sampled point y_n with the mean of W that is equal to 0. However, due to I, s_n has to be decoded to compare with I, which is just the Inter-Symbol Interference (ISI) [23] calculated by

$$
\begin{aligned}
I &= \sum_{l=0}^{L-1} \sum_{\substack{i=-\infty \\ i \neq 0}}^{\infty} s_{n+i} C_{l,i} \\
&= \sum_{l=0}^{L-1} \sum_{i=-\infty}^{-1} s_{n+i} C_{l,i} + \sum_{l=0}^{L-1} \sum_{i=1}^{\infty} s_{n+i} C_{l,i} \\
&= I_{past} + I_{future}. \quad (11)
\end{aligned}
$$

The use of I as the decoding threshold is to eliminate ISI. As can be seen from Eq. (11), I is decided by both the past symbols transmitted and the future symbols to be transmitted, and, as well as, by the channel parameters. For the practical communication system, the future symbols cannot be predicted, so, the I_{past} is used as the suboptimal threshold to decode the information. The channel information can be identified using channel estimation from the Sync probe signal in practical communication situation. The nth information bit is recovered by

$$
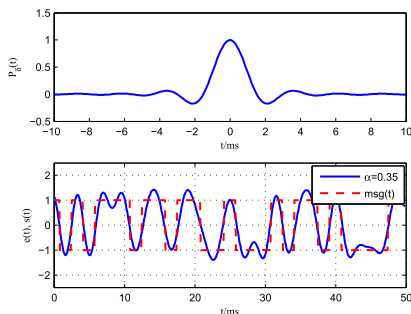\tilde{b}_n = \begin{cases} 1, & y_n > I_{past} \\ 0, & y_n \leq I_{past}, \end{cases} \quad (12)
$$

FIGURE 5. (a) Root cosine shape-forming filter waveform with bit rate r_b = 600 *bps*, sampling frequency f_s = 9.6 *kHz*, and roll-off factor γ = 0.35; **(b)** Filter output waveform for the symbol sequence [1 − 11 − 11, 11 − 111, −111 − 1 − 1, 1 − 1 − 1 − 11, −111 − 11, −1 − 1 − 1 − 11].

where $\tilde{b}_n$ is the nth recovered bit at the receiver, and y_n is the nth sampling point with maximal signal-to-noise ratio from the matched filter output $y(t)$. This operation eliminates the ISI caused by the past transmitted symbols. Although this operation does not remove all ISI, it does improve the communication performance when it is compared with the conventional one, as shown by the following simulations.

V. THE EXPERIMENTAL CONFIGURATION AND PERFORMANCE COMPARISON

In this Section, the conventional radio wave communication system is compared with the proposed chaotic radio wave communication system. As we have mentioned in the Introduction, one of the main aims of this work is to use chaos in conventional wireless communication system with minimal change to the system configuration. We only replace the shape-forming filter and the matched filter in the conventional wireless communication system with the chaotic shape-forming filter given in Eqs. (1) and (2); at the same time, we replace the matched filter at the receiver with the corresponding matched filter given by Eq. (6). In the conventional radio wave communication system, the square root raised cosine shape-forming filter and its corresponding matched filter are used [27], [28], as given by

$$P_\delta(t) = 4\gamma \frac{\cos\left(\frac{(1+\gamma)\pi t}{T_s}\right) + \frac{\sin\left(\frac{(1-\gamma)\pi t}{T_s}\right)}{4\gamma t/T_s}}{\pi\sqrt{T_s}\left(1 - (4\gamma t/T_s)^2\right)}, \quad (13)$$

where γ is roll-off factor and T_s is the symbol period. The time domain waveform and the filter output for the symbol sequence [1 − 11 − 11, 11 − 111, −111 − 1 − 1, 1 − 1 − 1 − 11, −111 − 11, −1 − 1 − 1 − 1] are shown in Fig. 5.

In the simulation, we use continuous-time manner to calculate Eqs. (1) and (2), in order to get continuous time baseband signal. The baseband signal is upconverted to the transmitted signal by using the DSBSC in Eq. (3). At the receiver, the continuous time demodulation signal and the continuous time filter output signal are obtained by passing the received signal through the Costas PLL, and then the discrete-time sampling points (with the maximum signal to noise ratio) from the filter output signal are used to compare with the suboptimal threshold in Eq. (12), instead of the optimal

threshold in Eq. (11) in order to recover the information bit. In the experiment, the above process is implemented by two TMS320C6713 Digital Signal Processor (DSP) to test the practical communication performance. In order to draw the effective Bit Error Rate (BER) curves for performance comparison, the practical wireless channel is replaced by a Rockwell hardware channel simulator, which is used to adjust the Signal-to-Noise Ratio (SNR) and the Doppler frequency shift. The baseband signal frequency range allowed by hardware equipment is limited from $300Hz$ to $3.3kHz$ and the sampling frequency of the analog-to-digital converter is $f_s = 9.6kHz$. The experimental setup is given in Fig. 6. At the transmitter, the bit transmission rate is 600 *bits/s* and the transmitted signal are grouped into frames, as shown in Fig. 7. The frame structure contains a Sync probe signal with 1024 bits and data information with 7170 bits, where the data information in each frame includes the baseband signal of 3585 bits generated by the CSF and SRRC.

Figure 8 shows the BER comparison under the single path wireless channel. Subplots (a) and (b) in Fig. 8 show the simulation and experimental results, respectively. Because it is the single path channel, no equalization is used in both methods. We can see from Fig. 8 that both simulation and experimental results are consistent, and both indicate that: firstly, the proposed CSF using suboptimal threshold achieves better BER performance than using zero as threshold; secondly, the BER performance of the CSF is inferior to the SRRC about 0.5dB in the single path channel. The reason is as follows. The ISI of CSF can be observed in the autocorrelation of the basis function, given by $y(t) = \int_{-\infty}^{\infty} p(\tau)p(t-\tau)d\tau$, as shown in Fig. 9. The normalized autocorrelation of CSF and SRRC are shown by blue solid line and red dashed line, respectively. The sampling point at the instant nT_s is the ISI of the current symbol to the nth ($n = \pm 1, \pm 2, \ldots$) symbol. It can be seen that the sampling points of the autocorrelation generated by SRRC at all instants nT_s are always zero, because it is designed to eliminate the ISI in single path channel. However, the ISI can be found in the autocorrelation of CSF at the same instant. It means that in a chaotic wireless communication system, although the receiver can also yield the maximum signal-to-noise ratio through the matched filter, the chaotic shape-forming filter itself cannot remove ISI influence in the single-path channel. For the first time, we point out and state that the chaotic baseband wireless communication is inferior to the conventional one in the single path channel. But we can see from Fig. 8 that the BERs of the proposed method and the conventional one are quite similar in the single path channel, because the suboptimal threshold is employed in the proposed method.

Figure 10 gives the two-path channel simulation and experimental BER comparison. The black line with down triangular mark and the green line with dot mark in the subplot (a) represent the simulation BER of the SRRC with and without the channel equalization using the minimum mean square error (MMSE) equalizer [29], respectively. The pink line with diamond mark, the blue line with up triangular
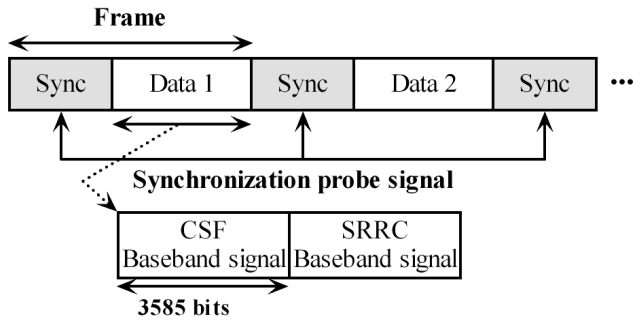
FIGURE 6. Experimental setup.

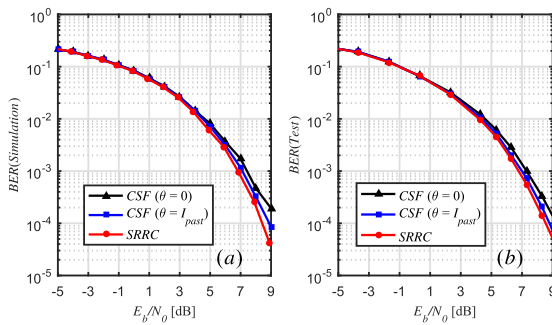**FIGURE 7.** The frame structure of the transmitted signal.

FIGURE 8. Simulation and experimental performance comparison of chaotic and conventional communication systems in single path channel, where the base frequency is $f = 0.6\ kHz$, sampling frequency is $f_S = 9.6\ kHz$, carrier frequency is $f_c = 1.8\ kHz$, and roll-off factor is $\gamma = 0.35$.
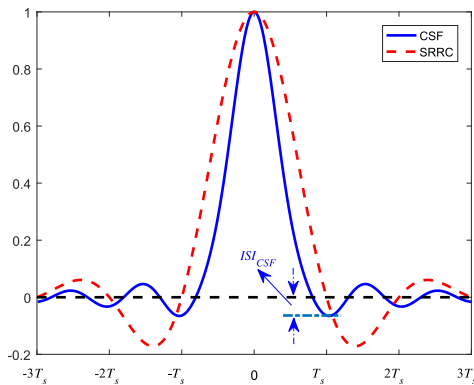

FIGURE 9. Normalized autocorrelation of CSF and SRRC.

FIGURE 10. Simulation and test performance comparison of chaotic and conventional communication systems in two-path channel, where the base frequency is $f = 0.6\ kHz$, sampling frequency is $f_S = 9.6\ kHz$, carrier frequency is $f_c = 1.8\ kHz$, and roll-off factor is $\gamma = 0.35$, delay time is $\tau = [0, T_S]$ (T_S is symbol period), attenuation coefficient is $\alpha_l = [1, 0.6]$; (a) The simulation BER performance comparison; (b) The test BER performance comparison.

FIGURE 11. Simulation result in the fast time-varying channel.

mark and the red line with rectangular mark, respectively, represents the simulation BER of the CSF using 0 as threshold, at the same time using the MMSE equalization, and using I_{past} as threshold without any equalization. Subplot (b) in Fig. 10 is the experimental BER corresponding
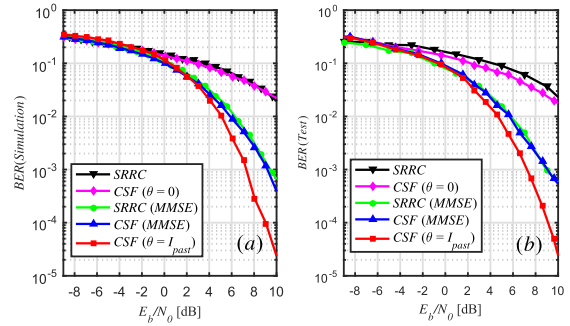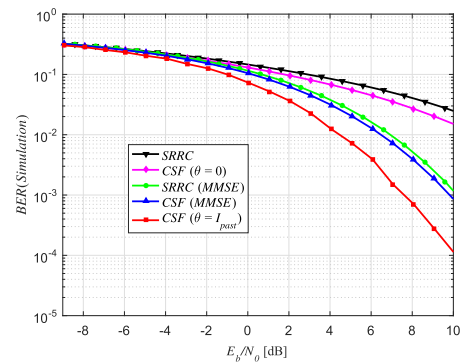
to Fig. 10(a). As can be seen from Fig. 10, under the multi-path channel, the simulation and the experimental test show that, when using I_{past} as the threshold, even without equalization, the BER of the chaotic one is lower than that of the SRRC even with MMSE. The chaotic communication system demonstrates better performance in the multi-path channel. For the other multi-path channel parameters, the results are similar to the results in Fig. 10. A point to be noticed here is that the channel parameters in the experiment are set as constant due to the Rockwell hardware device limitation, and the same channel parameters are set in the simulation to ensure a consistency between the simulations and the experiments. This setting is reasonable, because the radio channel is a slow time-varying channel. The channel parameters can be considered as constant in the coherence time, that is, in a frame signal. Moreover, various fast

time-varying multi-path channels parameters are also used to test the communication performance, as shown in Fig. 11. In the simulation, a three-ray multipath channel is considered, in which the attenuation coefficient follows a normal distribution with the mean values as [0.6, 0.3, 0.1], the variance of 0.05 and the delay time follows a uniformly distributed random process from 0 to $2T_s$, respectively. It can be seen that the BER performance comparison in the fast time-varying channel shows similar conclusions as the simulation results in Fig. 10.

VI. CONCLUSION

In this paper, in order to look for a better way to use chaos properties in the radio wave communication system with minimum modification to the conventional communication system, we propose to use the chaotic shape-forming filter and its corresponding matched filter to replace the conventional shape-forming filter. This new wireless communication system achieves maximum SNR, and the use of a simple suboptimal threshold improves the BER performance in multi-path channel, and improves the system performance in a simple way by removing the complicated channel equalization algorithm, thus simplifying the software of the system. In this work, an application of wireless communication with chaos are implemented in two DSPs with hardware channel simulator, exploring the engineering application of chaotic communication. Moreover, the chaotic shape-forming filter and the matched filter can be easily used in the 5G or 6G communication systems, because the shape-forming of the baseband signal is essential in a communication system. This work focus on improving the communication performance in complex channel in the sense of providing a lower BER as compared to the conventional one. The use of chaos in the proposed method cannot directly improve the communication security. However, it can be extended to spread spectrum communication to achieve a higher communication security [30].

REFERENCES

[1] E. Ott, C. Grebogi, and J. A. Yorke, "Controlling chaos," *Phys. Rev. Lett.*, vol. 64, no. 11, pp. 1196–1199, Mar. 1990.

[2] L. M. Pecora and T. L. Carroll, "Synchronization in chaotic systems," *Phys. Rev. Lett.*, vol. 64, no. 8, pp. 821–824, Feb. 1990.

[3] S. T. Hayes, C. Grebogi, and E. Ott, "Communication with chaos," *Phys. Rev. Lett.*, vol. 70, pp. 3031–3034, May 1993.

[4] K. M. Cuomo and A. V. Oppenheim, "Circuit implementation of synchronized chaos with applications to communications," *Phys. Rev. Lett.*, vol. 71, no. 1, pp. 65–68, Jul. 1993.

[5] V. Milanovic and M. E. Zaghloul, "Improved masking algorithm for chaotic communications systems," *Electron. Lett.*, vol. 32, no. 1, pp. 11–12, Jan. 2002.

[6] A. Abel and W. Schwarz, "Chaos communications-principles, schemes, and system analysis," *Proc. IEEE*, vol. 90, no. 5, pp. 691–710, May 2002.

[7] T. Yang and L. O. Chua, "Secure communication via chaotic parameter modulation," *IEEE Trans. Circuits Syst. I: Fundam. Theory Appl.*, vol. 43, no. 9, pp. 817–819, Sep. 1996.

[8] T. H. Shake, "Security performance of optical CDMA against eavesdropping," *J. Lightw. Technol.*, vol. 23, no. 2, pp. 655–670, Feb. 2005.

[9] M. Rahmati, R. Petroccia, and D. Pompili, "In-network collaboration for CDMA-based reliable underwater acoustic communications," *IEEE J. Ocean. Eng.*, vol. 44, no. 4, pp. 881–894, Oct. 2019.

[10] H. Dedieu, M. P. Kennedy, and M. Hasler, "Chaos shift keying: Modulation and demodulation of a chaotic carrier using self-synchronizing Chua's circuits," *IEEE Trans. Circuits Syst. II, Analog Digit. Signal Process.*, vol. 40, no. 10, pp. 634–642, Oct. 1993.

[11] X. Cai, W. Xu, L. Wang, and G. Kolumbán, "Multicarrier *M*-ary orthogonal chaotic vector shift keying with index modulation for high data rate transmission," *IEEE Trans. Commun.*, vol. 68, no. 2, pp. 974–986, Feb. 2020.

[12] M. P. Kennedy, G. Kolumbán, G. Kis, and Z. Jako, "Performance evaluation of FM-DCSK modulation in multipath environments," *IEEE Trans. Circuits Syst. I, Fundam. Theory Appl.*, vol. 47, no. 12, pp. 1702–1711, Dec. 2000.

[13] G. Zhang, Y. Wang, and T. Q. Zhang, "A novel QAM-DCSK secure communication system," *J. Comput. Inf. Syst.*, vol. 11, no. 8, pp. 2989–2999, Apr. 2015.

[14] W. Hu, L. Wang, and G. Kaddoum, "Design and performance analysis of a differentially spatial modulated chaos shift keying modulation system," *IEEE Trans. Circuits Syst. II, Exp. Briefs*, vol. 64, no. 11, pp. 1302–1306, Nov. 2017.

[15] H.-P. Ren, H.-P. Yin, C. Bai, and J.-L. Yao, "Performance improvement of chaotic baseband wireless communication using echo state network," *IEEE Trans. Commun.*, early access, Jul. 7, 2020, doi: 10.1109/TCOMM.2020.3007757.

[16] C. Bai, H.-P. Ren, and G. Kolumban, "Double-sub-stream M-ary differential chaos shift keying wireless communication system using chaotic shape-forming filter," *IEEE Trans. Circuits Syst. I, Reg. Papers*, early access, May 22, 2020, doi: 10.1109/TCSI.2020.2993674.

[17] A. Argyris, D. Syvridis, L. Larger, V. Annovazzi-Lodi, P. Colet, I. Fischer, J. García-Ojalvo, C. R. Mirasso, L. Pesquera, and K. A. Shore, "Chaos-based communications at high bit rates using commercial fibre-optic links," *Nature*, vol. 438, no. 7066, pp. 343–346, Nov. 2005.

[18] C. Williams, "Chaotic communications over radio channels," *IEEE Trans. Circuits Syst. I, Fundam. Theory Appl.*, vol. 48, no. 12, pp. 1394–1404, Dec. 2001.

[19] H.-P. Ren, M. S. Baptista, and C. Grebogi, "Wireless communication with chaos," *Phys. Rev. Lett.*, vol. 110, no. 18, May 2013, Art. no. 184101.

[20] H.-P. Ren, C. Bai, J. Liu, M. S. Baptista, and C. Grebogi, "Experimental validation of wireless communication with chaos," *Chaos, Interdiscipl. J. Nonlinear Sci.*, vol. 26, no. 8, Aug. 2016, Art. no. 083117.

[21] N. J. Corron, R. M. Cooper, and J. N. Blakely, "Analytically solvable chaotic oscillator based on a first-order filter," *Chaos, Interdiscipl. J. Nonlinear Sci.*, vol. 26, no. 2, Feb. 2016, Art. no. 023104.

[22] C. Bai, H. P. Ren, and C. Grebogi, "Experimental phase separation differential chaos shift keying wireless communication based on matched filter," *IEEE Access*, vol. 7, no. 1, pp. 25274–25287, Feb. 2019.

[23] J.-L. Yao, C. Li, H.-P. Ren, and C. Grebogi, "Chaos-based wireless communication resisting multipath effects," *Phys. Rev. E, Stat. Phys. Plasmas Fluids Relat. Interdiscip. Top.*, vol. 96, no. 3, Sep. 2017.

[24] J.-L. Yao, Y.-Z. Sun, H.-P. Ren, and C. Grebogi, "Experimental wireless communication using chaotic baseband waveform," *IEEE Trans. Veh. Technol.*, vol. 68, no. 1, pp. 578–591, Jan. 2019.

[25] N. J. Corron, J. N. Blakely, and M. T. Stahl, "A matched filter for chaos," *Chaos, Interdiscipl. J. Nonlinear Sci.*, vol. 20, no. 2, Jun. 2010, Art. no. 023123.

[26] E. Y. Zhang, *Mathematical Model of Short-Wave Channel, Shortwave Communication Technology*. Beijing, China: National Defense Industry Press, 2002, pp. 23–24.

[27] Q. Q. Shen and D. S. Zhu, *The Composition and Basic Principle of Single—Side Band Communication System, Shortwave Communications*. Xi'an, China: Xi'an Univ. of Electronic Science and Technology Press, 1989, pp. 42–60.

[28] C. X. Fan and L. N. Cao, *The Design of No Intersymbol Interference Transmission Characteristics, Principles of Communications*. Beijing, China: National Defense Industry Press, 2016, pp. 148–150.

[29] M. Tuchler, A. C. Singer, and R. Koetter, "Minimum mean squared error equalization using *a priori* information," *IEEE Trans. Signal Process.*, vol. 50, no. 3, pp. 673–683, Mar. 2002.

[30] H.-P. Ren, C. Bai, Q. Kong, M. S. Baptista, and C. Grebogi, "A chaotic spread spectrum system for underwater acoustic communication," *Phys. A, Stat. Mech. Appl.*, vol. 478, no. 15, pp. 77–92, Jul. 2017.
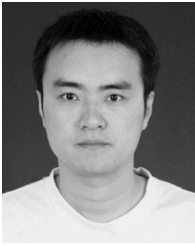
CHAO BAI was born in Xi'an, China, in 1988. He received the B.S. degree in automation from Xi'an Polytechnic University, in 2010, and the M.S. and Ph.D. degrees in control science and engineering from the Xi'an University of Technology, in 2014 and 2019, respectively. He holds a postdoctoral position at Xi'an Technological University. He has published more than ten journal articles and held three patents. His current research interests include chaotic communication and complex networks.

WU-YUN ZHENG was born in Inner Mongolia, China, in 1988. He received the B.S. degree in physics from the Shaanxi University of Technology, in 2011, and the M.S. degree in control science and engineering from the Xi'an University of Technology, in 2018. His current research interest includes chaotic communication in engineering applications.

HAI-PENG REN (Member, IEEE) was born in Heilongjiang, China, in March 1975. He received the Ph.D. degree in power electronics and power drives from the Xi'an University of Technology, Xi'an, China, in 2003. He worked as a Visiting Researcher in the field of nonlinear phenomenon of power converters with Kyushu University, Japan, from April 2004 to October 2004. He worked as Post Ph.D. Research Fellow of time-delay systems with Xi'an Jiaotong University from December 2005 to December 2008. He worked as an Honorary Visiting Professor in communication with chaos and complex networks with the University of Aberdeen, U.K., from July 2010 to July 2011. From December 2008 to June 2018, he worked as a Professor at the Department of Information and Control Engineering, Xi'an University of Technology. In July 2018, he moved to Xi'an Technological University. His research interests include nonlinear system control, complex networks, and communication with nonlinear dynamics.

CELSO GREBOGI was born in Curitiba, Brazil, in 1947. He received the B.S. degree from the Universidade Federal do Parana, Parana, Brazil, in 1970, and the M.S. and Ph. D. degrees from the University of Maryland, College Park, in 1975 and 1978, respectively.

His current research interests include systems biology, neurodynamics, methods to control chaos, the dynamics of spatio-temporal systems, active processes in chaotic flows, relativistic quantum dynamical systems, and nanosystems, including graphene and opto-mechanical systems. He is a Fellow of the Royal Society of Edinburgh, the Academia Europaea, the Brazilian Academy of Sciences, the World Academy of Sciences, the American Physical Society, and the Institute of Physics. As one of the participants, he proposed the famous O. G. Y. method for chaos control. In addition, he was listed in the Thomson Reuters Citation Laureates in 2016.

• • •